

## Experimental Studies of $\text{Os}^-$ : Observation of a Bound-Bound Electric Dipole Transition in an Atomic Negative Ion

René C. Bilodeau and Harold K. Haugen\*

*Department of Physics and Astronomy, McMaster University, Hamilton, Ontario, Canada L8S 4M1*

(Received 21 December 1999)

The first experimental studies of  $\text{Os}^-$  reveal the presence of two very strong resonances. One state is a narrow shape resonance lying only 3.52(12) meV above the ground state detachment threshold, while the other is bound by 11.48(12) meV. Convincing evidence that these states have odd parity is presented, making  $\text{Os}^-$  the only known atomic negative ion with bound states of opposite parity. Additionally, the binding energies for the  $\text{Os}^-$  ground state ( $^4F_{9/2}^e$ ) and first excited state ( $^4F_{7/2}^e$ ) are measured to be 1.077 80(12) eV and 0.553(3) eV, respectively.

PACS numbers: 32.80.Gc, 32.10.Hq, 32.70.Cs, 32.80.Dz

A number of atomic negative ion states remain poorly known or even completely unknown, despite considerable ongoing theoretical and experimental efforts [1–3]. For example, until now no experimental studies had been conducted on the negative ion of osmium. In fact, until very recent calculations [4], the knowledge of  $\text{Os}^-$  was limited to the semiempirical extrapolated estimate of 1.1(2) eV for the electron affinity (EA) of Os [3]. In addition to important applications [1,3], negative ions are of considerable interest on a fundamental level. Unlike neutral atoms and positive ions, which are bound by the Coulomb potential, negative ions are bound by a short range potential, more akin to a nuclear potential but on an atomic scale. Consequently, very few states (often only one term) are bound in the negative ion potential, in sharp contrast to the infinite number of bound states in other atomic systems. To date, bound-bound transitions observed in negative ions are always between levels from the same configuration and are thus electric dipole ( $E1$ ) forbidden, making experimental studies very challenging [5]. Over the past few decades considerable effort has been invested into finding an atomic negative ion with opposite parity bound states [3,6]. Although a number of theoretical studies indicated that  $\text{Cs}^-$  was a strong candidate for opposite parity bound states, recent detailed experimental studies eliminated this possibility [7] and left very few good potential systems [6].

This Letter reports the findings of the first experimental studies of  $\text{Os}^-$ . Infrared laser photodetachment indicates the presence of an unexpected pair of odd parity states in  $\text{Os}^-$ . One state is slightly unbound by only 3.52(12) meV, making it the lowest lying continuum feature ever observed in an atomic negative ion [7]. The other state is bound by 11.48(12) meV and is thus the most weakly bound state in an atomic negative ion observed to date [3]. More importantly, since the only other bound configuration of  $\text{Os}^-$  has even parity,  $\text{Os}^-$  is the only known negative ion with opposite parity bound states. This discovery offers a close to a long-standing question in atomic physics.

The experimental apparatus is described in detail elsewhere [8]. A Nd:YAG pumped dye laser, operating at a

10 Hz repetition rate with an  $\approx 8$  ns temporal width, is Raman shifted in a high pressure  $\text{H}_2$  cell to produce the tunable infrared light required in the experiments. The collimated laser light is sent through a  $\text{CaF}_2$  viewport into an ultrahigh vacuum chamber where it crosses at  $90^\circ$  with an 8 keV, 150 nA beam of  $\text{Os}^-$ , extracted from a Cs sputter source utilizing a high purity solid metal Os cathode. Using crossed polarizers, the laser pulse energies could be controllably tuned from under 20  $\mu\text{J}$  to over 3 mJ, while preserving the spatial and temporal characteristics of the laser pulse.

A schematic energy level diagram of  $\text{Os}^-$  and Os is presented in Fig. 1, based on the present experiments and very recent calculations by Norquist and Beck [4]. The relative cross section for detachment obtained from a scan covering  $850\text{ cm}^{-1}$  near the EA defining  $5d^7 6s^2 4F_{9/2}^e \rightarrow 5d^6 6s^2 5D_4^e$  detachment threshold is shown in Fig. 2. Two very strong peaks are evident from this scan: a “narrow peak” located near  $8600\text{ cm}^{-1}$  and a “wide peak” located near  $8700\text{ cm}^{-1}$ . Figure 3a shows the data from a high resolution scan covering a range around the narrow peak. The shape is consistent with a Lorentzian profile having a line center at  $8600.42(15)\text{ cm}^{-1}$  [ $1.066\ 316(19)\text{ eV}$ ] (using  $1\text{ eV} = 8065.544\ 77(32)\text{ cm}^{-1}$  [9]) and a full width at half maximum (FWHM) of  $0.166(3)\text{ cm}^{-1}$ , approximately the bandwidth of the laser. A similar high resolution scan around the wide peak (Fig. 3b) shows that this peak also has a Lorentzian shape, but is slightly asymmetric.

The Wigner law has been shown to accurately describe the threshold detachment behavior of a large number of negative ions [3,8,10,11]. The removal of a  $d$  electron results in an outgoing  $p$ -wave electron giving rise to a cross section following a  $3/2$  power law (the  $f$  wave is not expected to contribute near threshold). However, the law poorly describes the threshold behavior in the present  $\text{Os}^-$  case, as seen by the dashed curve in Fig. 2. This is due to the presence of the large shape resonance just above the threshold. A similar shape resonance was seen in (metastable)  $\text{He}^-$  due to the presence of the excited  $\text{He}^- 1s2p2p'^4P^e$  state lying less than 11 meV above the

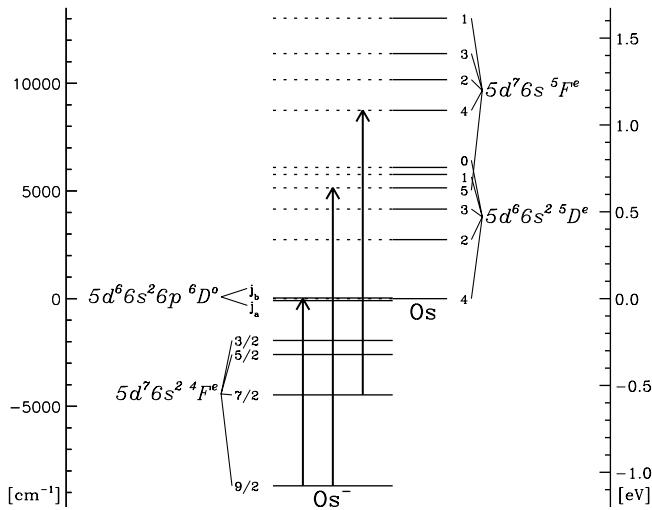


FIG. 1. Energy level diagram for  $\text{Os}^-$ . Arrows indicate the three measured thresholds. A tentative designation for the new ionic states is included.

$1s2s2p^4P^o \rightarrow 1s2p^3P^o$  threshold [12]. In that experiment, the Wigner law was also found to be inadequate, even very near to the detachment threshold. However, for photon energies  $\varepsilon$  greater than the threshold energy  $\varepsilon_0$ , the following equation was found to have excellent agreement with the observations [12,13]:

$$\sigma = a_0 + c(\varepsilon - \varepsilon_0)^{3/2} / [(\varepsilon - \varepsilon_r)^2 + (\Gamma/2)^2], \quad (1)$$

where  $c$  is a constant,  $\varepsilon_r$  is the resonance position, and  $\Gamma$  is the FWHM parameter of the resonance. Below threshold ( $\varepsilon < \varepsilon_0$ )  $\sigma$  equals the background  $a_0$ .

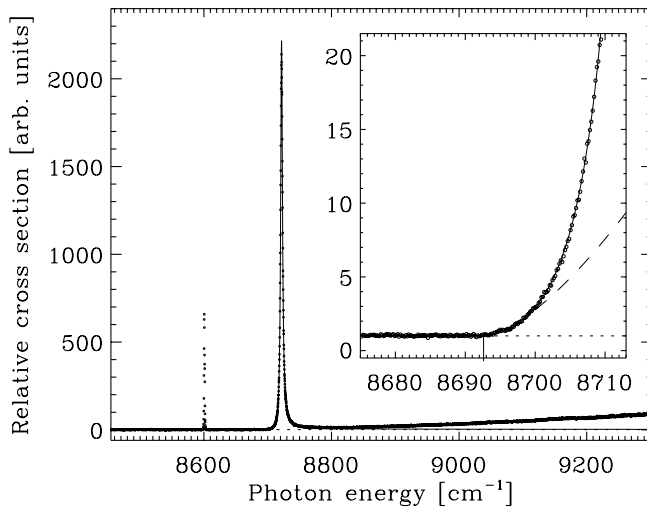


FIG. 2. Photodetachment of  $\text{Os}^-$ . Inset: High resolution scan around the ground state threshold, fitted to Eq. (1) (solid curve) and the Wigner law (long-dashed curve). The scale is normalized to the background signal (short dashes), due to small amounts of excited  $\text{Os}^- 4F^e$  ions in the beam. The data have been corrected for variations in pulse energies (between 0.4 and 0.7 mJ per pulse) over this range.

The resonance parameters  $\varepsilon_r = 8721.4(3) \text{ cm}^{-1}$  [ $1.08132(4) \text{ eV}$ ] and  $\Gamma = 3.66(3) \text{ cm}^{-1}$  are obtained from the fit of Eq. (1) to the data of Fig. 3b. To obtain an accurate value for the threshold position, Eq. (1) is fit to the high resolution scan shown in the inset in Fig. 2, with the two resonance parameters held fixed to the determined values. The threshold position is determined to be  $8693(1) \text{ cm}^{-1}$  [ $1.07780(12) \text{ eV}$ ], consistent with  $1.048 \text{ eV}$ , calculated by Norquist and Beck [4]. Although this model agrees very well with the data near the threshold, it is clear from Fig. 2 that the function deviates from the data at photon energies  $\approx 8750 \text{ cm}^{-1}$  and higher. In particular, Eq. (1) predicts that the cross section should approach zero with increasing photon energy, while the data increase toward higher photon energies. A deviation from Eq. (1) at higher photon energies is not unexpected, as this function is expected to hold only near the threshold [12]. However, three possible explanations, in addition to the possible breakdown of Eq. (1), can be considered: (i) the presence of yet another resonance at even higher photon energies, (ii) the opening of a new detachment channel from one of the excited states of  $\text{Os}^-$ , or (iii) signal from the detachment of impurity ions possibly present in the ion beam. The saturation arguments discussed below suggest that the signal observed over the entire range of Fig. 2 originates from the same population, indicating that possibilities (ii) and (iii) are very unlikely. Also, although the resolution of the mass analyzing magnet (better than  $\approx 4\%$ ) is not sufficient to eliminate near-mass coincident molecular ion impurities (e.g.,  $\text{OsH}^-$ ), the relative size of the features did not vary in measurements carried out over a few months. Moreover, the very narrow and isolated features observed here are not characteristic of signals obtained from molecular ions. Finally, since the structures appear precisely in the expected threshold

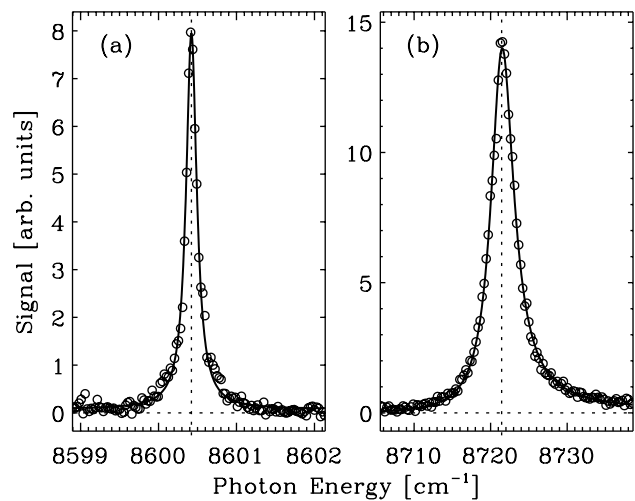


FIG. 3. High resolution scans of (a) the bound-bound resonant transition (narrow peak) and (b) the shape resonance (wide peak), obtained at relatively low pulse energies ( $\approx 0.4 \text{ mJ}$  per pulse) to avoid saturation broadening.

region and  $\text{Os}^-$  is such a prolific ion from a sputter source, we consider it very unlikely that impurity ions could account for the observed signals.

To confirm the position of the  $\text{Os}^-$  ground state, a  $400\text{ cm}^{-1}$  scan around the  $5d^7 6s^2 4F_{9/2}^e \rightarrow 5d^7 6s^2 5F_5^e$  threshold was conducted, locating this threshold at  $13\,800(80)\text{ cm}^{-1}$ . This determines the binding for  $\text{Os}^- 4F_{9/2}^e$  to be  $8660(80)\text{ cm}^{-1}$ , in agreement with the above value. Finally, the  $4F_{7/2}^e \rightarrow 5F_4^e$  threshold was observed at  $13\,205(24)\text{ cm}^{-1}$ ; thus the binding of  $\text{Os}^- 4F_{7/2}^e$  is  $4462(24)\text{ cm}^{-1}$  [ $0.553(3)\text{ eV}$ ]. (The larger uncertainties obtained are a consequence of the large backgrounds observed when detaching to excited neutral states.) The measurement of the  $4F_{9/2}^e$  level sets the  $4F_{9/2}^e - 4F_{7/2}^e$  fine structure splitting to  $4231(25)\text{ cm}^{-1}$  [ $0.525(3)\text{ eV}$ ], which agrees within  $15\text{ meV}$  to the theoretical splitting of  $0.540\text{ eV}$  [4].

Given the very large range of signal strengths and relatively large cross sections observed, due consideration of signal saturation is warranted. Although saturation of the detector and electronics can be easily avoided by careful selection of sensitivity ranges, saturation by depletion of the ion population in the interaction region is also possible. We therefore observed the saturation behavior of the detachment signal at three different photon energies: (a) at the maximum of the narrow peak, (b) at the maximum of the wide peak, and (c) at high photon energies ( $9300\text{ cm}^{-1}$ ). At each photon energy, the intensity of the laser light was varied. Assuming uniform illumination and ion density in the interaction region, the signal  $N$  obtained from a single photon detachment process with cross section  $\sigma_b$ , follows the relation [14]

$$N = N_0(1 - e^{-\sigma_b P}), \quad (2)$$

where  $N_0$  is a constant equal to the maximum signal that would be detected if all the ions were detached, and depends on the ion density, the ion-laser overlap, the efficiency of the detector, and the amplification of the detection electronics. If we assume the ions are stationary over the duration of the laser pulse  $\tau \approx 8\text{ ns}$ , then  $P = \int \Phi dt = E_p / Sh\nu$  is the number of photons per unit area, where  $\Phi$  is the photon flux,  $E_p$  is the laser pulse energy, and  $S$  is the area of the laser beam cross section. Figure 4 is a plot of the signal measured over a large range of pulse energies at the three wavelengths. The solid curve (b) is the best fit result of Eq. (2) to the data points obtained at the maximum of the wide peak (b). The excellent agreement between the data and this model confirms that the detachment process is indeed due to absorption of a single photon into an excited  $\text{Os}^-$  state with subsequent autodetachment. In contrast, this function does not describe the data obtained at the maximum of the narrow peak (a) for pulse energies  $\lesssim 1\text{ mJ}$  (long-short broken curve in Fig. 4). In fact, at low pulse energies, the shape of the curve approaches that of a quadratic function, indicating the absorption of two photons. With

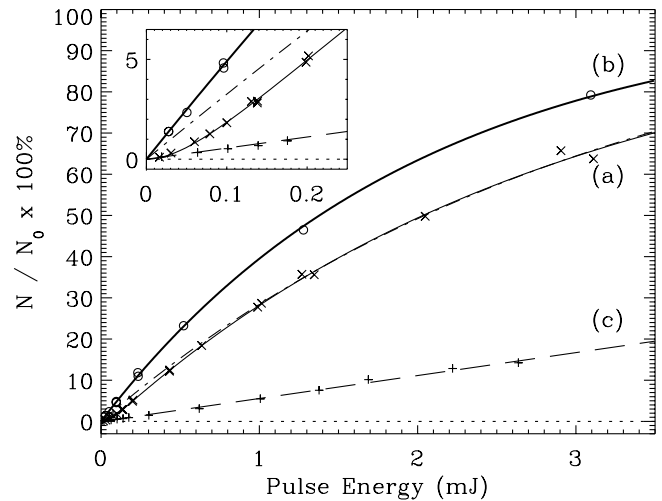


FIG. 4. Percent of population detached versus pulse energy, observed at (a) the maximum of the narrow peak, (b) the maximum of the wide peak, and (c) high photon energies. [For clarity of presentation, the signal for (c) has been multiplied by a factor of 5.] The fitted curves are described in the text. Inset: Expanded view of the low pulse-energy data.

the current experimental parameters, a standard rate-equation approach [15] can be used to determine the signal dependence on pulse energy for a resonant two-photon process. Given  $\sigma_a$  and  $\sigma_d$ , the cross sections for the resonant and detachment steps, respectively, we obtain

$$N = N_0 \left( 1 - \frac{\sigma_{(+)} e^{-\sigma_{(-)} P} - \sigma_{(-)} e^{-\sigma_{(+)} P}}{\sigma_{(+)} - \sigma_{(-)}} \right), \quad (3)$$

where  $\sigma_{(\pm)} = \frac{1}{2}(2\sigma_a + \sigma_d) \pm \frac{1}{2}\sqrt{4\sigma_a^2 + \sigma_d^2}$ . As can be seen from the solid curve (a) in Fig. 4, this model describes the data very well. The value of the maximum signal amplitude  $N_0$  obtained is the same (within the uncertainty of 10%) as that obtained from the wide peak, which confirms that the signal is derived from the same initial state of  $\text{Os}^-$ , i.e., the ground state. The high photon energy signal (c) is also consistent with an unsaturated signal originating from the  $\text{Os}^-$  ground state.

For an accurate determination of the cross sections  $\sigma_a$ ,  $\sigma_b$ , and  $\sigma_d$ , a more detailed model and more precise determination of the laser pulse and ion beam characteristics would be necessary. However, the approximations made are sufficiently accurate to obtain order of magnitude estimates for these quantities. For  $S \approx 0.4\text{ cm}^2$ , we obtain [16]  $\sigma_a \sim 6 \times 10^{-16}\text{ cm}^2$ ,  $\sigma_d \sim 5 \times 10^{-17}\text{ cm}^2$ , and  $\sigma_b \sim 4 \times 10^{-17}\text{ cm}^2$ . The Einstein  $A$  coefficient for a resonant transition is related to the resonant cross section  $\sigma$  by  $A \approx 4\pi^2 \sigma \Gamma / \lambda^2$ , where  $\lambda$  is the resonant wavelength [15]. With  $\Gamma = 0.17$  and  $3.7\text{ cm}^{-1}$ , we have  $A \sim 10^4\text{ s}^{-1}$  for both resonances. We can also obtain an estimate of  $A$  for the bound-bound transition (narrow peak) by comparing the signal level obtained in this experiment with that obtained from other resonant transitions (of known strengths) observed with this apparatus [5]. If we assume

that the detaching step has the same cross section in all cases, we deduce  $A \sim 10^5 \text{ s}^{-1}$  for the bound-bound transition. All known magnetic dipole transitions have  $A$  coefficients at least 100 times smaller than these [5,17] (when properly scaled for wavelength [15]), thus ruling out a same-parity transition. In fact, although the transition strength appears to be somewhat weak for a fully allowed  $E1$  transition, strengths of  $\sim 10^4$  or  $\sim 10^5 \text{ s}^{-1}$  fall squarely within the expected range of values for a spin forbidden  $E1$  transition at these wavelengths, in heavy elements such as Os [17]. This is therefore convincing evidence that the excited states have opposite parity to the ground state of  $\text{Os}^-$ . Finally, since the narrow resonance appears at lower energies than the ground state of Os, we conclude that it is bound. The requirement that these states have odd parity suggests that they may have a  $5d^6 6s^2 6p$  or  $5d^7 6s 6p$  configuration. Preliminary calculations by Beck [18] for the binding of a  $p$  electron to neutral Os show that  $5d^6 6s^2 6p$  lies about  $4000 \text{ cm}^{-1}$  below  $5d^7 6s 6p$ , indicating that the excited states may be due to the attachment of a  $p$  electron to the ground state of Os. Given the approximate  $A$  coefficients obtained, and since conservation of angular momentum requires that  $J = 7/2, 9/2,$  or  $11/2$  for both levels, we can deduce that the only two likely terms from this configuration are  ${}^6D$  and  ${}^6F$ . The calculations by Beck confirm that the  $5d^6 6s^2 6p$  state is mostly  ${}^6D$  ( $\approx 75\%$ ) and  ${}^6F$  ( $\approx 15\%$ ) in character, with the remainder being largely  ${}^4F$  in character. We therefore suggest  $5d^6 6s^2 6p {}^6D^o$  as a likely designation for the new levels.

In conclusion, we have discovered two excited ionic states of odd parity in the negative ion of osmium. This makes  $\text{Os}^-$  the only known atomic negative ion with bound states of opposite parity. Also, our preliminary investigations of  $\text{W}^-$  indicate similar continuum resonances in that system. These discoveries strongly suggest that a wealth of interesting structure remains to be discovered in the transition metal negative ions.

We gratefully acknowledge the Natural Science and Engineering Research Council of Canada (NSERC) for support of this work. We thank M. Scheer for numerous insightful comments, T. Andersen, R.L. Brooks, and V.V. Petrunin for helpful discussions, and D.R. Beck for providing his preliminary results.

*Note added.*—The increase in the detachment signal at higher photon energies (Fig. 2) is explained by a breakdown of Eq. (1) and can be accurately described by a more detailed model. These results will be published in a separate article.

---

\*Also with the Department of Engineering Physics, McMaster University, Ontario, Canada.

[1] S.J. Buckmann and C.W. Clark, *Rev. Mod. Phys.* **66**, 539 (1994); C. Blondel, *Phys. Scr.* **T58**, 31 (1995), and references therein.

- [2] V.K. Ivanov, *J. Phys. B* **32**, R67 (1999).
- [3] H. Hotop and W.C. Lineberger, *J. Phys. Chem. Ref. Data* **14**, 731 (1985); T. Andersen, H.K. Haugen, and H. Hotop, *J. Phys. Chem. Ref. Data* **28**, 1511 (1999).
- [4] P.L. Norquist and D.R. Beck, *Phys. Rev. A* **61**, 014501 (2000).
- [5] M. Scheer, H.K. Haugen, and D.R. Beck, *Phys. Rev. Lett.* **79**, 4104 (1997); M. Scheer, R.C. Bilodeau, C.A. Brodie, and H.K. Haugen, *Phys. Rev. A* **58**, 2844 (1998); M. Scheer, R.C. Bilodeau, and H.K. Haugen, *J. Phys. B* **31**, L11 (1998).
- [6] Theoretical studies suggest that there may be opposite parity bound states in some lanthanides and actinides: S.H. Vosko, J.B. Lagowski, I.L. Mayer, and J.A. Chevary, *Phys. Rev. A* **43**, 6389 (1991); D. Datta and D.R. Beck, *Phys. Rev. A* **50**, 1107 (1994); K. Dinov, D.R. Beck, and D. Datta, *Phys. Rev. A* **50**, 1144 (1994). However, the claims have not been confirmed [A.M. Covington, D. Calabrese, J.D. Thompson, and T.J. Kvale, *J. Phys. B* **31**, L855 (1998)].
- [7] M. Scheer, J. Thøgersen, R.C. Bilodeau, C.A. Brodie, H.K. Haugen, H.H. Andersen, P. Kristensen, and T. Andersen, *Phys. Rev. Lett.* **80**, 684 (1998), and references therein.
- [8] M. Scheer, C.A. Brodie, R.C. Bilodeau, and H.K. Haugen, *Phys. Rev. A* **58**, 2051 (1998).
- [9] P.J. Mohr and B.N. Taylor, *J. Phys. Chem. Ref. Data* (to be published).
- [10] M. Scheer, R.C. Bilodeau, C.A. Brodie, and H.K. Haugen, *Phys. Rev. A* **58**, 2844 (1998); R.C. Bilodeau, M. Scheer, and H.K. Haugen, *J. Phys. B* **31**, 3885 (1998); P.L. Norquist, D.R. Beck, R.C. Bilodeau, M. Scheer, R.A. Sawley, and H.K. Haugen, *Phys. Rev. A* **59**, 1896 (1999).
- [11] R.C. Bilodeau, M. Scheer, H.K. Haugen, and R.L. Brooks, *Phys. Rev. A* **61**, 012505 (2000).
- [12] J.R. Peterson, Y.K. Bae, and D.L. Huestis, *Phys. Rev. Lett.* **55**, 692 (1985); C.W. Walter, J.A. Seifert, and J.R. Peterson, *Phys. Rev. A* **50**, 2257 (1994); C.A. Ramsbottom and K.L. Bell, *J. Phys. B* **32**, 1315 (1999).
- [13] V.A. Esaulov, *Ann. Phys. (Paris)* **11**, 493 (1986).
- [14] H. Hotop and W.C. Lineberger, *J. Chem. Phys.* **58**, 2379 (1973); P. Balling, C. Brink, T. Andersen, and H.K. Haugen, *J. Phys. B* **25**, L565 (1992).
- [15] See, for example, R. Loudon, *The Quantum Theory of Light* (Oxford, New York, 1983), 2nd ed.
- [16] Note that two pairs of roots for  $\sigma_a$  and  $\sigma_d$  are possible for any given pair of parameters  $\sigma_{(+)}$  and  $\sigma_{(-)}$ . The second pair of solutions,  $\sigma_a \sim 2 \times 10^{-17} \text{ cm}^2$  and  $\sigma_d \sim 2 \times 10^{-15} \text{ cm}^2$ , is rejected because  $2 \times 10^{-15} \text{ cm}^2$  is 2 or 3 orders of magnitude larger than expected for a detachment cross section in an atomic negative ion (barring strong continuum resonance enhancements) [2,13,14].
- [17] A.A. Radzig and B.M. Smirnov, *Reference Data on Atoms, Molecules, and Ions* (Springer-Verlag, New York, 1985); J.R. Fuhr, G.A. Martin, and W.L. Wiese, *J. Phys. Chem. Ref. Data* **17**, 1 (1988).
- [18] D.R. Beck (private communication).